

## Heavy ion transfer reactions: Status and perspectives

L CORRADI

INFN-Laboratori Nazionali di Legnaro – Viale dell’Universita’ 2-35020,  
Legnaro (Padova), Italy  
E-mail: corradi@lnl.infn.it

**Abstract.** With the large solid angle magnetic spectrometer (PRISMA) coupled to the  $\gamma$ -array (CLARA), extensive investigations of nuclear structure and reaction dynamics have been carried out. In the present paper aspects of these studies will be presented, focussing more closely on the reaction mechanism, in particular on the properties of quasielastic and deep inelastic processes and on measurements at energies far below the Coulomb barrier.

**Keywords.** Multinucleon transfer; coupled channels; magnetic spectrometers.

**PACS Nos** 25.70.Hi; 29.30.Aj; 24.10-i; 23.20.Lv

### 1. Introduction

Multinucleon transfer reactions at Coulomb barrier energies is an important field of research in low-energy heavy-ion physics [1]. Through this mechanism one can in fact investigate nucleon–nucleon correlation in nuclei, the transition from the quasielastic to the deep inelastic regime and channel coupling effects in sub-barrier fusion reactions. Different aspects of the correlation between reaction channels have been extensively discussed at the recent Fusion06 [2] and Fusion08 [3] conferences. An important and still poorly investigated question is what are the relevant degrees of freedom acting in the transfer process, i.e. single nucleon, pair or even cluster transfer modes. Thanks to the recent development of high-resolution and high-efficiency experimental set-ups, one could unambiguously detect in mass and charge the nuclei produced in transfer reactions up to the pick-up of six neutrons and the stripping of six protons (see e.g. [4,5] and references therein). The advent of the large solid angle magnetic spectrometer (PRISMA) [6] allowed the increase in detection limit by more than an order of magnitude, with a significant gain in mass resolution for very heavy ions. Further, the coupling of this spectrometer to the large  $\gamma$ -array (CLARA) [7] allowed to perform  $\gamma$ -particle coincidences, thus detecting the transfer strength to the lowest excited levels of binary products and performing gamma spectroscopy for nuclei moderately far from the stability produced via nucleon transfer or deep inelastic reactions, especially in the neutron-rich region. These studies are of primary importance for reactions which are to be done

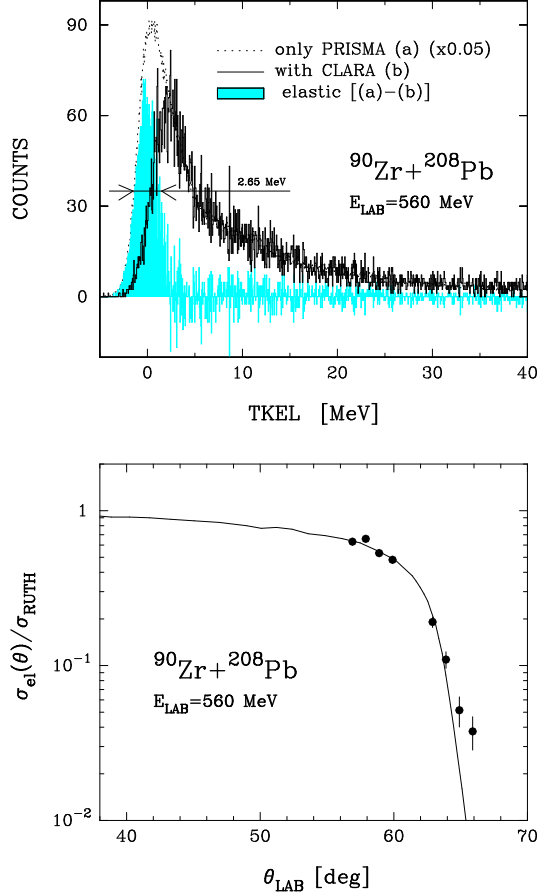


**Figure 1.** Top: Experimental angle integrated total kinetic energy loss distributions (TKEL) for  $^{90}\text{Zr}$  in the  $^{90}\text{Zr} + ^{208}\text{Pb}$  reaction (a) without coincidence with  $\gamma$ -rays and (b) with at least one  $\gamma$ -ray detected in CLARA. The two spectra are normalized in such a way that the high TKEL tails match. The gray area corresponds to the subtraction between the two spectra [(a)–(b)]. Bottom: Experimental (points) and GRAZING calculated (curve) differential cross-section for elastic scattering, normalized to Rutherford.

with radioactive ion beams, where multinucleon transfer has been shown to be a competitive tool for the study of neutron-rich nuclei, at least for certain mass regions. In this paper the focus will be on specific aspects of reaction mechanism studies being performed with PRISMA.

## 2. Elastic scattering

Elastic scattering is important to learn about the (outer part of) nuclear potential and provides essential information on absorptive effects, to be accounted for in

coupled channel calculations. The present set-up offers the possibility to separate elastic from inelastic scattering, at least for some nuclei. The pure elastic scattering can be determined by comparing the events with and without  $\gamma$ -coincidences [8]. As an example, in the top panel of figure 1 are shown the total kinetic energy loss (TKEL) spectra for  $^{90}\text{Zr}$  in the reaction  $^{90}\text{Zr}+^{208}\text{Pb}$  with and without  $\gamma$ -coincidence, normalized in the tail (large TKEL) region. By subtraction, one obtains the pure elastic contribution. This subtracted spectrum is characterized by a narrow peak centred at  $\text{TKEL} \simeq 0$  MeV with an FWHM of 2.65 MeV. Moreover, its centroid is separated by 2.15 MeV from the maximum of the TKEL spectrum in coincidence with CLARA, whose value is very close to the inelastic excitation of the first  $2^+$  state in  $^{90}\text{Zr}$ . Such a procedure should be reliable, provided that the shape of the spectrum in coincidence with  $\gamma$ -rays only weakly depends on the  $\gamma$  multiplicity. By repeating this subtraction in steps of one degree over the entrance angular range ( $\Delta\theta_{\text{lab}} = 12^\circ$ ) of PRISMA, one obtains the elastic angular distribution whose ratio to Rutherford is shown in the bottom panel of figure 1, in comparison to the results of GRAZING calculations [9] (see also the next section). The very pronounced fall-off of the elastic cross-section for large angles clearly indicates that the elastic scattering for this system is dominated by strong absorption. The good agreement between theory and experiment gives us confidence on the used potential and on the fact that the included reaction channels correctly describe the depopulation of the entrance channel (absorption). A similar kind of analysis has been successfully done for the  $^{48}\text{Ca} + ^{64}\text{Ni}$  system [10].

### 3. Total cross-sections

Total angle and  $Q$ -value integrated cross-sections for multineutron and multiproton transfer channels have been investigated in various systems close to the Coulomb barrier [1]. Recently, such measurements have been extended with heavy ions detected in PRISMA, for instance, in the reactions  $^{90}\text{Zr} + ^{208}\text{Pb}$  and  $^{40}\text{Ca} + ^{96}\text{Zr}$  [8,11]. Both projectiles and targets are closed shell and therefore ideal candidates for a quantitative comparison with theoretical models [12,13]. One observes events corresponding to the pick-up as well as the (weaker) stripping of neutrons. Isotope identification in the proton transfer direction is visible down to  $(-8p)$  stripping, but it is sensitive enough to observe more proton stripping channels. Note that in the quasielastic regime only proton stripping and neutron pick-up are favoured from optimum  $Q$ -value arguments.

Figure 2 shows, as an example, the experimental total cross-sections for the pure neutron pick-up channels in  $^{90}\text{Zr} + ^{208}\text{Pb}$  and  $^{40}\text{Ca} + ^{96}\text{Zr}$  systems and the channels involving the one-proton stripping in  $^{40}\text{Ca} + ^{96}\text{Zr}$ . The data are compared with calculations performed with the semiclassical code GRAZING [9]. The treatment of the transfer degrees of freedom is based on the assumption that in a heavy-ion collision the exchange of a nucleon proceeds via many open channels that are all quite weak, so that they may be treated independently. GRAZING treats surface degrees of freedom and particle transfer on the same footing and the exchange of many nucleons proceeds via a multistep mechanism of single nucleons (both protons and neutrons, via stripping and pick-up processes). The trajectory is calculated by solving the system of classical equations for the variables of relative motion and the

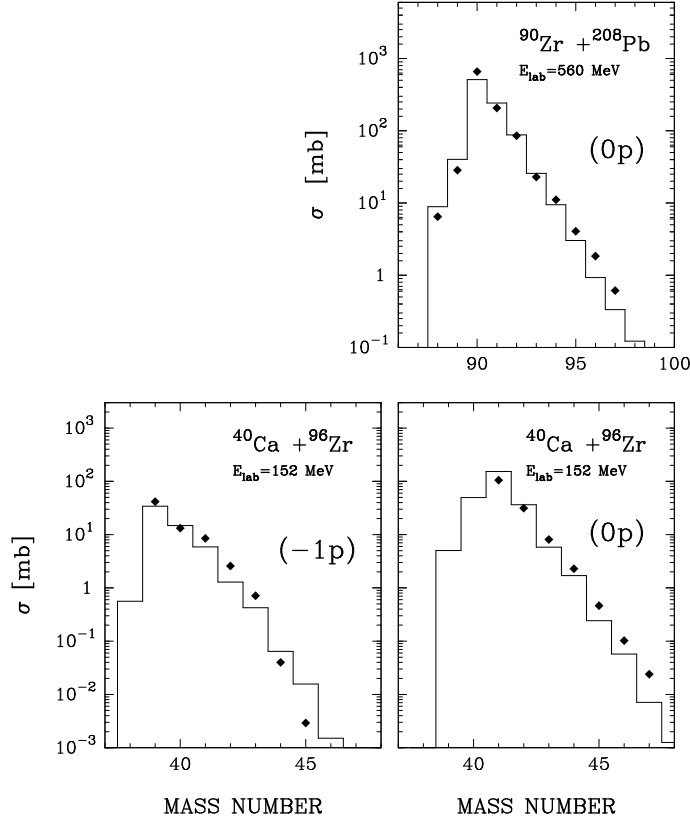


**Figure 2.** Total cross-sections for pure neutron pick-up channels in the  $^{90}\text{Zr} + ^{208}\text{Pb}$  reaction. Bottom: Total cross-sections for pure neutron pick-up (right panel) and one-proton stripping (left panel) channels in the  $^{40}\text{Ca} + ^{96}\text{Zr}$  reaction. The points are the experimental data and the histograms are the GRAZING code calculations (see text).

deformation parameters for the surface modes. The model includes the low-lying  $2^+$  and  $3^-$  states of both projectile and target and the corresponding giant resonances. This model has been successfully applied in the description of multinucleon transfer reactions [1] and can reproduce the near-barrier fusion excitation functions and extracted barrier distributions [14,15].

Looking at the experimental data of figure 2 one finds that the cross-sections for the neutron pick-up decrease by almost a constant factor for each transferred neutron, as an independent particle mechanism would suggest. The comparison with calculations supports this idea. One notices a remarkable agreement both in the neutron pick-up as well as on the neutron stripping side. One can mention that the pure proton cross-sections behave differently, with the population of the  $-2p$  channel as strong as the  $-1p$  channel. This suggests the contribution of processes involving the transfer of proton pairs in addition to the successive transfer of single protons. One also observes that as more protons are transferred, the average mass

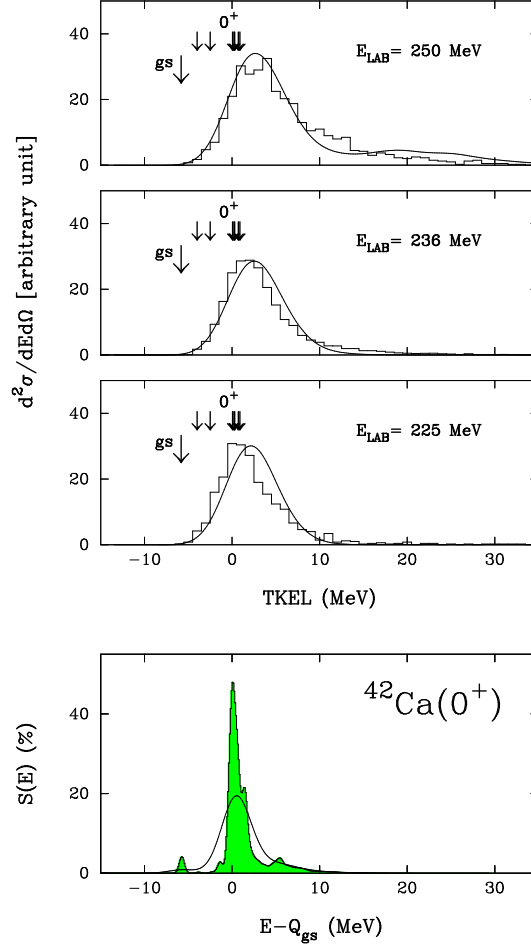
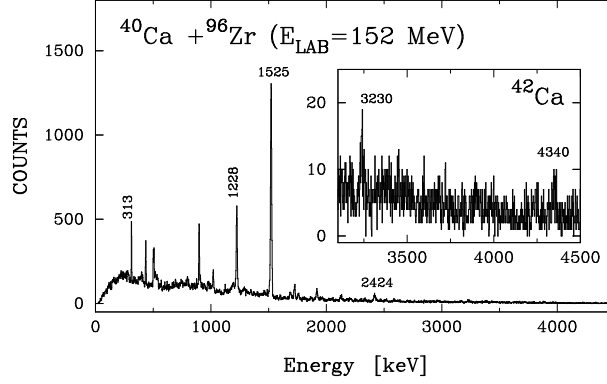


**Figure 3.** Experimental (histograms) and theoretical (curves) total kinetic energy loss distributions of the two-neutron pick-up channels at the indicated energies. The arrows correspond to the energies of  $0^+$  states in  $^{42}\text{Ca}$  with an excitation energy lower than 7 MeV. Bottom panel shows the strength function  $S(E)$  from shell model calculations.

shifts to lower neutron number. This is attributed, at least partly, to the effect of neutron evaporation from the primary fragments. This effect of neutron evaporation is indirectly visible from the analysis of refs [4,5] and has been also directly seen with PRISMA+CLARA by means of cross coincidences (see later).

#### 4. Pairing vibrations

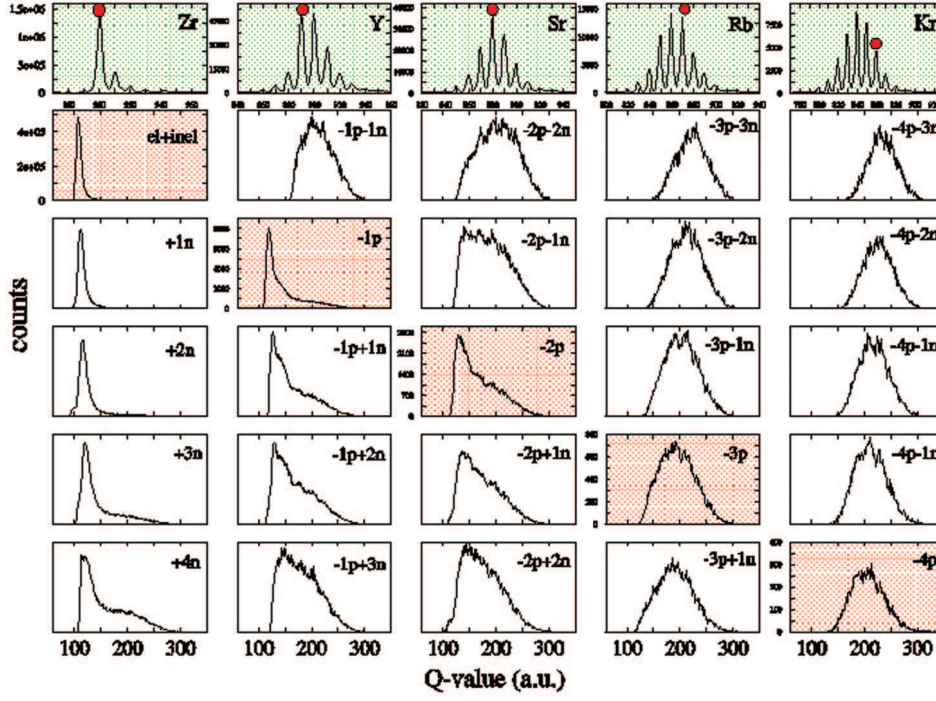
Closed-shell systems are well suited for the identification of states reached via the addition and/or the removal of pairs of nucleons. Those states have been studied



**Figure 4.**  $\gamma$ -ray spectrum with expanded region in the inset for  $^{42}\text{Ca}$  obtained in the  $^{40}\text{Ca} + ^{96}\text{Zr}$  reaction.

with light ion reactions and formed the basis for the identification of pairing vibration degrees of freedom in the nuclear medium [16]. With heavy ions, interesting expectations are coming by looking at the  $Q$ -value distributions of the recently measured  $^{40}\text{Ca} + ^{208}\text{Pb}$  reaction [17]. Figure 3 shows the TKEL distributions at three bombarding energies for the two-neutron pick-up channel in comparison with calculations. As can be seen, the two-neutron pick-up channel displays at all measured energies a well-defined maximum, which, within the energy resolution of the experiment, is consistent with the dominant population, not of the ground state of  $^{42}\text{Ca}$ , but of states with an excitation energy of around 6 MeV. The inspection of this population for the  $+2n$  channel tells us that the maximum of the distributions correspond to the transfer of two neutrons in the  $p_{3/2}$  orbital, and we remind that the single-particle form-factors for the  $p_{3/2}$  orbital is much larger than the one for the  $f_{7/2}$  orbital that constitutes the main configuration of the ground state of  $^{42}\text{Ca}$ . The  $(p_{3/2})^2$  configuration corresponds to the main component of the excited  $0^+$  states at around 5.8 MeV of excitation energy that were interpreted as multi (additional and removal) pair-phonon states [16]. The strong concentration of strength near 6 MeV of peculiar  $0^+$  states for  $^{42}\text{Ca}$  (they must contain the  $(p_{3/2})^2$  configuration) is clearly visible in the bottom part of figure 3, where the strength distribution  $S(E)$  from large-scale shell model calculations is shown. These results open, at least in our expectation, the possibility to study multipair-phonon excitations.

The PRISMA + CLARA set-up should allow the observation of the decay pattern of the populated  $0^+$  states. In figure 4 we show the  $\gamma$ -spectrum for  $^{42}\text{Ca}$  obtained in the reaction  $^{40}\text{Ca} + ^{96}\text{Zr}$  [8]. We observe here (see expanded region) a  $\gamma$ -transition at 4340 keV which is consistent with the decay from a level at 5.8 MeV to the  $2_1^+$  state. The limited statistics accumulated for this transition (such high-energy  $\gamma$ -rays have a low photopeak efficiency) does not allow to deduce the spin of the populated level, though the distribution over the rings of CLARA shows an isotropic pattern but with very large error bars. In the expanded  $\gamma$ -spectrum we also observe a  $\gamma$ -transition of 3230 keV, which is the main branch of the decay from the  $2^+$  state at 4760 keV, strongly populated in  $(t, p)$  reactions.

**$^{90}\text{Zr} + ^{208}\text{Pb}$  E=560 MeV PRISMA**

**Figure 5.** TKEL spectra obtained in the reaction  $^{90}\text{Zr} + ^{208}\text{Pb}$  for the indicated transfer channels. In the top row are shown the mass distribution associated with the different nuclear charges, while the circles indicate the specific masses corresponding to the spectra displayed along the upper-left/lower-right diagonal. The centroid of the elastic + inelastic channel corresponds to  $Q = 0$ . The scale of the  $Q$ -value axis is 1 MeV/channel.

### 5. From quasielastic to deep inelastic regime

The  $Z$  and  $A$  identification capability and the large detection efficiency of PRISMA allows to follow the evolution of the reaction from the quasielastic (i.e. few-nucleon transfer and low TKEL) to the deep inelastic regime (i.e. many-nucleon transfer and large TKEL). Here, the challenging question is to what extent the fundamental degrees of freedom (single particle, surface and pair modes) used to describe a few-nucleon transfer processes, holds in the presence of large energy losses and/or large number of nucleons. In figure 5, the TKEL spectra obtained in the  $^{90}\text{Zr} + ^{208}\text{Pb}$  reaction for different transfer channels are shown. One can follow the evolution pattern as a function of the number of transferred neutrons and protons. For instance, in the case of pure neutron transfer one sees a quasielastic peak and an increasing strength on large energy loss components when adding neutrons. Note that with PRISMA one detects secondary fragments and that the TKEL spectra are constructed by assuming binary reactions. For channels which, due

to optimum  $Q$ -values, are not directly populated, the shape of the corresponding TKEL differs a lot from the smooth behaviour just described. Look for instance at the comparison between the  $(-1p+1n)$  channel (mainly directly populated) and the  $(-1p-1n)$  one. This different behaviour tends to smooth out with a larger number of transferred protons.

Large energy losses are associated with nucleon evaporation from the primary fragments. The importance of neutron evaporation in the modification of the final yield distribution was outlined in inclusive measurements [4,5]. These effects can be directly seen with PRISMA + CLARA. Gating with PRISMA on a specific  $Z$  and  $A$  (light partner) the velocity vector of the undetected heavy partner can be evaluated and applied for the Doppler correction of its corresponding  $\gamma$ -rays. In those spectra not only the  $\gamma$ -rays belonging to the primary binary partner are

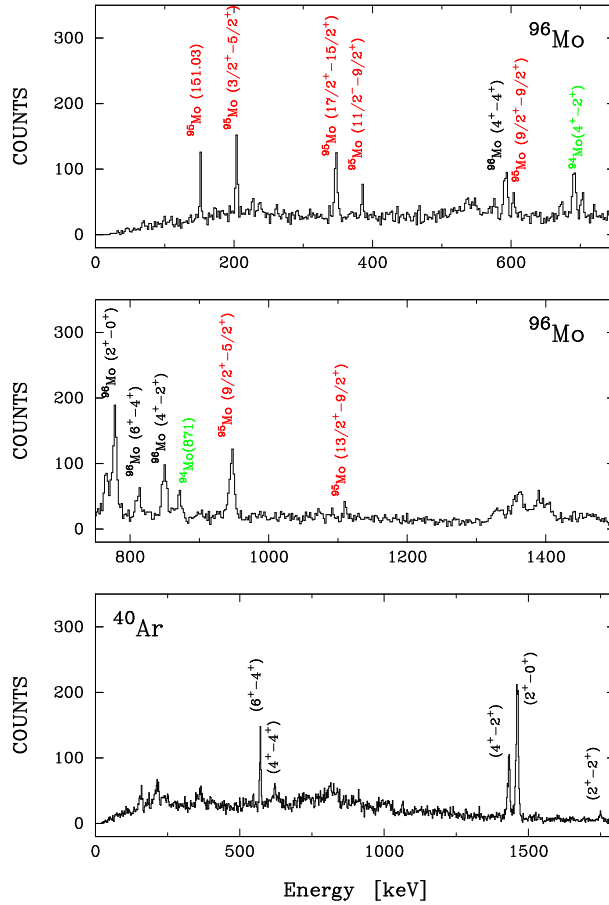


**Figure 6.**  $\gamma$ -spectra for the  $-2p+2n$  channel in the reaction  $^{40}\text{Ca} + ^{96}\text{Zr}$  Doppler corrected for the heavy (top two panels) and light fragments (bottom panel). To have a better identification of the different  $\gamma$ -lines for the heavy fragment we used an expanded energy scale.



present but also the ones produced after evaporation takes place. An example is given in figure 6 for the  $-2p+2n$  channel populated in the  $^{40}\text{Ca} + ^{96}\text{Zr}$  reaction [8]. About 60% of the yield corresponds to the primary  $^{96}\text{Mo}$ , while the rest is equally shared between isotopes corresponding to the evaporation of one and two neutrons. In general, for a few-nucleon transfer channels most of the yield corresponds to the true binary partner. This behaviour is closely connected with the observed TKEL. For the neutron pick-up channels the major contribution in the TKEL is close to the optimum  $Q$  values ( $Q_{\text{opt}} \simeq 0$ ), while in the proton stripping channels larger TKEL are observed, thus the neutron evaporation has a stronger effect on the final mass partition.

## 6. Sub-barrier transfer reactions

In recent years there has been growing interest in studying dynamic processes at energies well below the Coulomb barrier, in particular the sub-barrier fusion [2,3]. This same energy range is also ideal to investigate transfer processes, which are strongly connected with fusion, as they probe different but complementary ranges of nuclear overlap. To set the frame, one can write the transfer cross-section as

$$\sigma_{\text{tr}} \sim e^{-2/\hbar \int W(r(t))dt} \sum \left| \int F_{if}(r(t)) e^{i\omega_{if}} dt \right|^2,$$

where the first exponential term gives the probability to remain in the elastic channel and the second describes the direct population of the transfer channels,  $F(r)$  being the transfer form factor and  $e^{i\omega_{if}}$  defining the  $Q$ -value window, with the sum running over all the final channels. The integrals are performed along the Coulomb trajectory. The imaginary potential  $W(r)$ , that describes the depopulation of the entrance channel, at very low energies is dominated by the single-nucleon transfer channels. Since the  $Q$ -value distributions get narrower at low bombarding energies, these sub-barrier studies may provide important information on the nuclear correlation close to the ground state. In this energy region the multinucleon transfer channels should be dominated by a successive mechanism with negligible contribution from a cluster-like transfer [18]. This fact should provide a simpler analysis of the data.

From the experimental point of view, measurements of heavy-ion transfer reactions at far sub-barrier energies have significant technical difficulties. At low bombarding energies, angular distributions result, in the centre of mass frame, in a strong backward peaking, with a maximum at  $\theta_{\text{cm}} \simeq 180^\circ$ . The absolute yield gets very small, and therefore high efficiency is needed. At the same time, mass and nuclear charge resolutions must be maintained at a level sufficient to distinguish the different reaction channels. For situations where the projectile has a significant fraction of the target mass, as it is in most cases, the backscattered projectile-like fragment has such a low energy that usual identification techniques become invalid. A suitable way to overcome these limitations is by means of inverse kinematics. Thus we recently detected multinucleon transfer channels in the reactions  $^{94,96}\text{Zr} + ^{40}\text{Ca}$  at different bombarding energies below the Coulomb barrier, making use of the PRISMA+CLARA set-up. The use of inverse kinematics and the

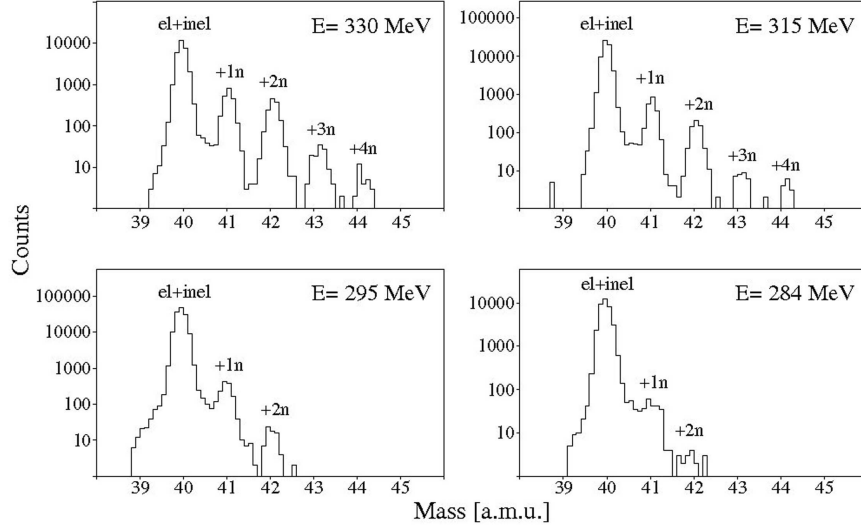


**Figure 7.** Mass distributions for pure neutron transfer channels obtained in the reaction  $^{94}\text{Zr} + ^{40}\text{Ca}$  at the indicated bombarding energies. Ca-like recoils have been detected at  $\theta_{\text{lab}}=20^\circ$  with the PRISMA spectrometer.

detection at very forward angles, allowed to have, at the same time, enough kinetic energy of the outgoing recoils (for energy and therefore mass resolution) and forward focussed angular distribution (high efficiency). Sub-barrier fusion cross-sections for the same system had been previously measured with high precision [19] and a complete set of data for both multinucleon transfer and fusion reactions would provide an excellent basis for coupled channel calculations.

The mass spectra for pure neutron transfer channels in the system  $^{94}\text{Zr} + ^{40}\text{Ca}$  obtained after trajectory reconstruction at four bombarding energies are shown in figure 7. While at higher energies, one observes the populations of up to four-nucleon transfer, at the lower energies (below the Coulomb barrier) only one- and two-neutron transfer survive. The  $Q$ -value distributions for the  $+2n$  channel at the lowest energies are very narrow and close to the ground state to ground state transition, as a result of the very low excitation energy of the transfer reaction products at these sub-barrier energies. The experimental results will be compared with coupled channel calculations, in particular the comparison of two-nucleon vs. one-nucleon transfer should provide information on nucleon–nucleon correlation effects.

## 7. Summary and outlook

In this paper, selected examples of the recently obtained results in the field of multinucleon transfer reactions at the Coulomb barrier are presented. New opportunities are offered by the implementation of large acceptance spectrometers based on trajectory reconstruction. With these devices one gained more than an order

of magnitude in the total efficiency while keeping good resolution for the detection of heavy-ion transfer products. Therefore, in coupling them with  $\gamma$ -arrays, one can study the transfer yield to specific final states and their decay modes. The experimental yields have been analysed with semiclassical theories developed to calculate at the same time quasielastic and deep inelastic processes. These theories have been able to provide a consistent description of transfer and fusion reactions by using a few degrees of freedom, surface modes and single particles. Much wider investigations in the field are required, for instance at sub-barrier energies where nuclei enter into contact through the long tail of the nuclear densities. It is in these regions that, for very neutron-rich nuclei, information on nucleon–nucleon correlation could be obtained by studying the excitation functions of specific transfer channels.

### Acknowledgements

The author wishes to acknowledge that this work is the result of a cooperative work of many people of the PRISMA+CLARA Collaboration belonging to different institutions (LNL, Padova, Torino, Zagreb, Bucharest, Strasbourg).

### References

- [1] L Corradi, G Pollarolo and S Szilner, *J. Phys.* **G36**, 113101 (2009)
- [2] *Fusion06: Int. Conf. on Reaction Mechanisms and Nuclear Structure at the Coulomb barrier*, S Servolo (Venezia), Italy, 19–23 March 2006, *AIP Proc. Ser.* edited by L Corradi *et al* (Melville, New York) Vol. 853
- [3] *Fusion08 : Int. Conf. on New Aspects of Heavy Ion Collisions Near the Coulomb Barrier*, Chicago (USA), September 22–26, 2008, *AIP Proc. Ser.* edited by K E Rehm *et al* (Melville, New York, 2009) Vol. 1098
- [4] L Corradi *et al*, *Phys. Rev.* **C66**, 024606 (2002)
- [5] S Szilner *et al*, *Phys. Rev.* **C71**, 044610 (2005)
- [6] A M Stefanini *et al*, *Nucl. Phys.* **A701c**, 217 (2002)
- [7] A Gadea *et al*, *Eur. Phys. J.* **A20**, 193 (2002)
- [8] S Szilner *et al*, *Phys. Rev.* **C76**, 024604 (2007)
- [9] A Winther, program GRAZING, <http://www.to.infn.it/~nanni/grazing>
- [10] D Montanari *et al*, *Acta Phys. Pol.* **B40**, 585 (2009)
- [11] L Corradi, *Nucl. Phys.* **A787**, 134 (2007)
- [12] A Winther, *Nucl. Phys.* **A572**, 191 (1994)
- [13] A Winther, *Nucl. Phys.* **A594**, 203 (1995)
- [14] G Pollarolo and A Winther, *Phys. Rev.* **C62**, 054611 (2000)
- [15] G Pollarolo, *Phys. Rev. Lett.* **100**, 252701 (2008)
- [16] R A Broglia, O Hansen and C Riedel, *Advances in nuclear physics* edited by M Baranger and E Vogt (Plenum, New York, 1973) Vol. 6, p. 287
- [17] S Szilner *et al*, *Eur. Phys. J.* **A21**, 87 (2004)
- [18] B F Bayman and J Chen, *Phys. Rev.* **C26**, 1509 (1982)
- [19] A M Stefanini *et al*, *Phys. Rev.* **C76**, 014610, (2007)